Transportation Research Part C 47 (2014) 139–154

Contents lists available at ScienceDirect

Transportation Research Part C

journal homepage: www.elsevier.com/locate/trc

Traffic volume forecasting based on radial basis function neural network with the consideration of traffic flows at the adjacent intersections

Jia Zheng Zhu [a,b], Jin Xin Cao [a,*], Yuan Zhu [c]

[a] Institute of Transportation, Inner Mongolia University, Hohhot 010070, PR China
[b] MOE Key Laboratory for Urban Transportation Complex Systems Theory and Technology, School of Traffic and Transportation, Beijing Jiaotong University, Beijing 100044, PR China
[c] Polytechnic Institute, New York University, NY 11201, USA

ARTICLE INFO

Article history:
Received 30 September 2013
Received in revised form 8 April 2014
Accepted 30 June 2014
Available online 31 July 2014

Keywords:
Traffic volume
Forecasting method
Data mining
Neural networks
Flocking phenomena
Missing data

ABSTRACT

The forecasting of short-term traffic flow is one of the key issues in the field of dynamic traffic control and management. Because of the uncertainty and nonlinearity, short-term traffic flow forecasting could be a challenging task. Artificial Neural Network (ANN) could be a good solution to this issue as it is possible to obtain a higher forecasting accuracy within relatively short time through this tool. Traditional methods for traffic flow forecasting generally based on a separated single point. However, it is found that traffic flows from adjacent intersections show a similar trend. It indicates that the vehicle accumulation and dissipation influence the traffic volumes of the adjacent intersections. This paper presents a novel method, which considers the travel flows of the adjacent intersections when forecasting the one of the middle. Computational experiments show that the proposed model is both effective and practical.

© 2014 Elsevier Ltd. All rights reserved.

1. Introduction

The traffic flow forecasting, especially the short-term traffic flow forecasting, has been recognized as a critical need for the intelligent transportation systems. It provides the theoretical and data supports for the traffic management systems, traveler information systems, emergency processing systems, and other related systems. On the one hand, Traffic Management Center (TMC) collects the traffic flow information to evaluate the real-time traffic condition of the road network, and to predict the traffic condition in the next moment by applying the short-term traffic flow forecasting techniques. The related information can be provided to the decision makers to adjust the route guidance strategy and other traffic management plans. On the other hand, the traffic information can be released to road users to efficiently assist them in choosing the travel route, the departure time, and the travel mode so as to avoid the traffic congestion (Stathopoulos and Karlaftis, 2003).

The short-term traffic flow forecasting means that the observation period is quite short, which is generally less than 15 min. The Highway Capacity Manual 2010 suggests using a 15-min traffic flow rate for operational analyses. In the past decades, a variety of models and methodologies have been applied to the traffic flow forecasting by researchers. There are two main trends in the area of traffic flow forecasting. One is to develop more efficient methodologies and models to fit different situations.

* Corresponding author. Tel./fax: +86 471 499 6004.
E-mail address: caojinxin@gmail.com (J.X. Cao).

http://dx.doi.org/10.1016/j.trc.2014.06.011
0968-090X/© 2014 Elsevier Ltd. All rights reserved.

Current model of the traffic flow forecasting involves two main approaches: parametric and non-parametric techniques (Vlahogianni et al., 2004). The famous model base on parametric technique, namely the Box–Jenkins model (ARIMA model) provides a perfect solution to most of the time-series problems. It is obviously that traffic volume values are time series data. And the ARIMA model was first introduced to the forecasting of traffic flow by Ahmed and Cook in 1979. Then the ARIMA model was proved to be a regular practice in time-series transportation data analysis, especially in traffic forecasting (Levin and Tsao, 1980; Davis et al., 1991; Hamed et al., 1995; Williams and Hoel, 2003; Stathopoulos and Karlaftis, 2003). Afterwards, researchers found that ARIMA model cannot tackle the problem of the extreme volume values forecasting (Davis et al., 1991; Hamed et al., 1995; Vlahogianni et al., 2004).

As for non-parametric models, the most widely used one is Artificial Neural Network (ANN), the one of Computational Intelligence (CI) models (Karlaftis and Vlahogianni, 2011). ANN has been widely used for forecasting of transportation data, especially the short-term traffic flow forecasting. The ANN is a nonlinear dynamic system, which is characterized in the parallel co-processing and distributed information storage. Although each individual neuron has very simple and limited function, the network consisting of a large number of neurons can achieve the functions are extremely abundant.

Multi-Layer Perception (MLP), Back-Propagation Neural Networks (BPNN) and Radial Basis Function Neural Networks (RBFNN) are the most widely used ANN models in short-term traffic flow forecasting (Karlaftis and Vlahogianni, 2011). Compared with BPNN, RBFNN required less network training time and showed better performance (Park et al., 1998). Amin et al. (1998) used the RBFNN to predict the traffic flow. Jayawardena and Fernando (1998) present an application of the RBFNN for hydrologic modeling and runoff simulation in a small catchment and report that it is more efficient computationally than the BP algorithm. Chen's research (2001) has also been shown that the RBF performed slightly better than the MLP. And the structure of RBFNN is simpler than MLP because it has only one hidden layer. Nevertheless there are some discussions about the structure of ANN. The 'black-box' structure of ANN was considered to hide from the user (Ripley, 1993, 1994). But for the traffic flow forecasting, we can take advantages of the structure to use the traffic volume of different locations to make prediction. On the contrary, the time series approach takes no account of the structural relationship that exists between one point and another.

Another trend is to develop more efficiency hybrid methods, specially the combination of the ANN and other methods. Hybrid ANN models were proved to forecast the traffic flow more efficiently. Van der Voort et al. (1996) proposed a hybrid model that combined Kohonen self-organizing maps with ARIMA models. The fuzzy-neural model was also applied to traffic flow forecasting (Yin et al., 2002). Bayesian combined neural network was proved to have better performance (Zheng et al., 2006). Genetic algorithms were also adopted to improve the performance of ANN (Abdulhai et al., 1999; Vlahogianni et al., 2005).

Although many different methodologies have been applied for the forecasting, the ultimate goal remains the same: to obtain the forecasting result more precisely and faster. Researchers also focused on improving and optimizing the existing methodologies and models. An object-oriented neural network was proposed for traffic forecasting through a time-lag recurrent network (Dia, 2001). Vlahogianni et al. (2008) proposed a multilayer strategy considering the temporal patterns by using the neural network approaches.

In recent years, data analysis based multi-section of road networks has become a hot issue in the area of traffic flow forecasting. Whittaker et al. (1997) used a number of different points' average speed and traffic volume to analyze the influence of each point in the road network in Netherlands. Williams (2001) forecast traffic flow through four traffic collection points near the city of Bonn, Germany. Stathopoulos and Karlaftis (2001) used the spectrum analysis and the cross-spectral analysis on the traffic flow in different locations. The result shows that the traffic volume of the section in different location has the character of autocorrelation and correlation. This correlation varied with different period and distance of different location. Kamarianakis and Prastacos (2003) demonstrated the application of univariate and multivariate techniques in an urban network using the data sets originating from a set of loop detectors.

Research about the multi-section traffic flow forecasting reveals that the traffic volumes of each collection points are significantly correlated. The intersections, as the node of road network, are easily to form the flock of vehicles. The accumulation and dissipation of one intersection obviously affect the state of traffic flow of adjacent intersections. We can exploit the spatio-temporal features of the volume of adjacent intersection to optimize the performance of the forecasting model. In this paper, a RBFNN-based method by using the traffic flow data of adjacent intersections is proposed to obtain more accurate forecasting result and to solve the problem of missing data.

2. RBF neural networks and the flocking phenomena

2.1. RBFNN for traffic flow forecasting

The Radial Basis Function Neural Network (RBFNN) is a three-layered feed-forward neural network with one radial basis layer. It can uniformly approximate any continuous function with a prospected accuracy. The RBFNN has local generalization abilities and fast convergence speed. The entire network includes three layers: an input layer, a nonlinear hidden layer (radial basis layer) and a linear output layer, as can be seen in Fig. 1.

Fig. 1 shows the typical structure of an n–h–m RBFNN, which has n inputs, h nodes of hidden layer, and m outputs. The vector $\mathbf{x} = (x_1, x_2, \cdots, x_n)^{\mathrm{T}} \in \mathbb{R}^n$ is the input vector of the network, and $\mathbf{W} \in \mathbb{R}^{h \times m}$ is the output weight matrix. The vector

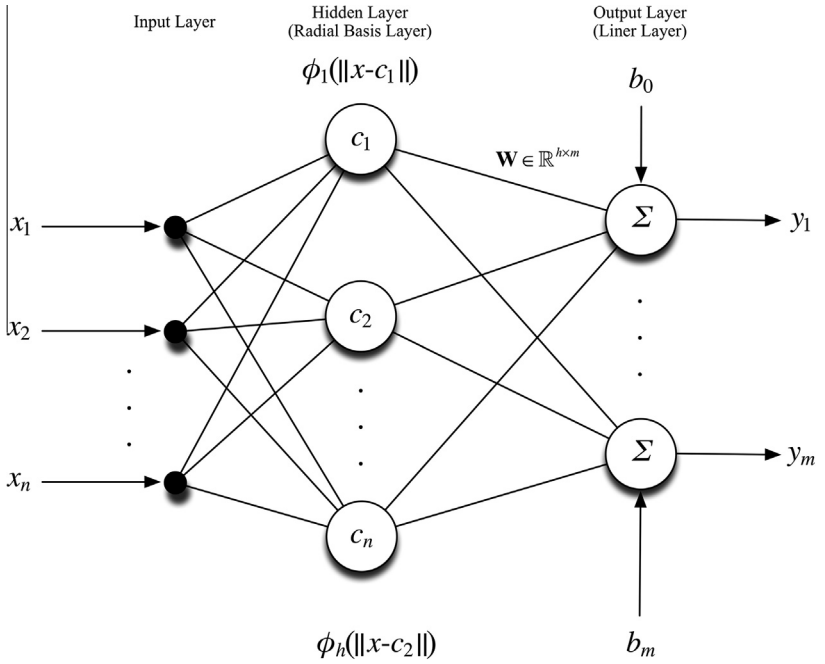

Fig. 1. The structure of RBFNN.

$\mathbf{y} = (y_1, y_2, \cdots, y_m)^{\mathrm{T}}$ is the output of the network, and $\phi_i(*)$ is the activation function of hidden node *i*. The notation Σ represents the linear activation function of a neuron in the output layer.

The node of the hidden layer generates partial reaction of the input signal. When the input signal is close to the center range of the base function, the nodes of hidden layer produce better output. Therefore, this network has a good capacity of local approximation. When it comes to the basis function, the Gauss function is most generally used:

$$R_i(x) = \exp\left[-\frac{\|x - c_i\|^2}{2\sigma_i^2}\right], \quad i = 1, 2, \ldots, m \tag{1}$$

As the previous study results shows, the unprocessed RBF model revealed apparent time-lag phenomena (Park, 2002). Park suggested to use the neuro-fuzzy based hybrid model to avoid the time-lag phenomena. Although this method is effective for normal traffic volume cases, it takes no account of the influence of road network and different measurement point.

2.2. The flocking phenomena

Flocking is a large number of individuals with the movement of the swarming phenomena. There are some typical examples of flocking, including birds, fish and bacterial community. Reynolds first proposed the model of flocking in 1987 (Reynolds, 1987). A model named Boid was developed to explore how computer animation simulate the behavior of flock of birds and flock of fish. Inspired by this biological flocking behavior research, researchers developed many basic theories and applications for the dynamic performance of many biological and engineering cluster behavior and control methods. It is a multi-disciplinary integration of biology, systems and control, mathematics, robotics, physics and computer science, such as the simulation of the multi-agent.

At present, there are two main approaches in research about flocking behavior (Li et al., 2008). One views the flock as a field, working with the density of the flock and deriving mean field properties. It can be useful for modeling the overall dynamics of large flocks (Toner and Tu, 1995). Another is to build an agent-based model following the individual agents (points or particles) that make up the flock. This approach is widely used because the individual particle models can follow information on heading and spacing (Carrillo et al., 2010). In this research, we concentrate more on the aggregate behaviors of the flocks formed near the intersection.

Helbing's research (2001) revealed that self-driven many-particle systems display a rich spectrum of spatio-temporal pattern formation phenomena. The flocks of bird, a representative of self-driven many-particle systems, may be assimilated to the flock of cars. As a typical spatio-temporal problem of traffic flow, short-term traffic flow forecasting could be modified based the very phenomenon by utilize the traffic flow data at different collecting point. At intersections various collective patterns of motion can be formed, for instance, the flocking of the vehicles gathered near the signalized intersections.

We are inspired by the biological phenomena that the group of cars on the road could be regard as flock. Vehicles need to move along roads and keep a minimum distances from each other. There is also a phenomenon of aggregation and dissipation in the flock of cars. As for the prediction of traffic volume, the traffic volume of upstream and downstream can be considered to be one of the factors for prediction (Dia, 2001). Vehicles easily form the flocks near intersections. Associate with the flocking phenomena, we think the change of traffic volume values in one intersection may have the save the similar trend with the adjacent intersections'. Within a certain distance, the traffic state at time period t may be in common with the traffic state of adjacent intersections at time period $t-1$. So use the traffic data of adjacent intersections may mitigate the effects of time-lag phenomena in traffic forecasting.

3. Case study

3.1. Data collection and analysis

The traffic volume data was collected by the loop detectors in Baotou City of China from September 17th to 19th, 2012, including 3 adjacent intersections along Shaoxian Rd., namely Shaoxian Rd. & Shifu West Rd., Shaoxian Rd. & Aerding Ave., and Shaoxian Rd. & Shifu East Rd. The distances between each two intersections are 312 m and 308 m, and locations of the loop detectors are shown in Fig. 2.

The traffic flow data are listed in Table A.1. The data includes 128 groups of continuous traffic volume of the three intersections. The time interval is set to be 15 min. Table 1 summarizes the descriptive statistics of the data set, where V_{max} represents the maximum of 15-min traffic flow rate during the observation period and V_{min} represents the minimum of 15-min traffic flow rate.

It can be observed that the data of the adjacent intersections show the similar trend during the observation period. Two curve fitting procedures of traffic volume data between each two intersections are conducted as can be seen from Figs. 3 and 4. The results of the goodness of fit are shown in Table 2, where $V_k(i)$ represents the traffic flow of Intersection k during period i (15 min).

From Figs. 3 and 4, it can be found that the traffic volumes of the adjacent intersections are linearly related within such a short distance of 500 m. The Pearson Correlation Coefficients of the volume data of each two intersections are calculated by applying Eq. (2), where $\overline{V}_k$ denotes the average traffic volume of Intersection k during the entire observation period. The correlations of both two intersections are significant at the 0.01 level, as can be seen in Table 3.

$$r=\frac{\sum_{i=1}^{n}\left[V_k(i)-\overline{V}_k\right]\left[V_2(i)-\overline{V}_2\right]}{\sqrt{\sum_{i=1}^{n}\left[V_k(i)-\overline{V}_k\right]^2}\sqrt{\sum_{i=1}^{n}\left[V_2(i)-\overline{V}_2\right]^2}},\quad k=1,3 \tag{2}$$

3.2. The improved forecasting model

Traditional prediction methods based on ANN generally apply to a single road or several sections of one road. Lin et al. put forward an idea by taking the advantages of the adjacent roads, which improve the prediction results by regarding the road system as a network (Lin et al., 2008). In this study, traffic volumes of the adjacent intersections are taken into consideration. The traffic volumes of the adjacent intersections are used as the input to obtain more accurate forecasting result.

We use 125 data sets of the 128 data sets for forecasting. Each group contains four groups of 15-min data. The first three groups of data are used as the input data, and the rest one is remained to check the accuracy. The first 100 groups are the

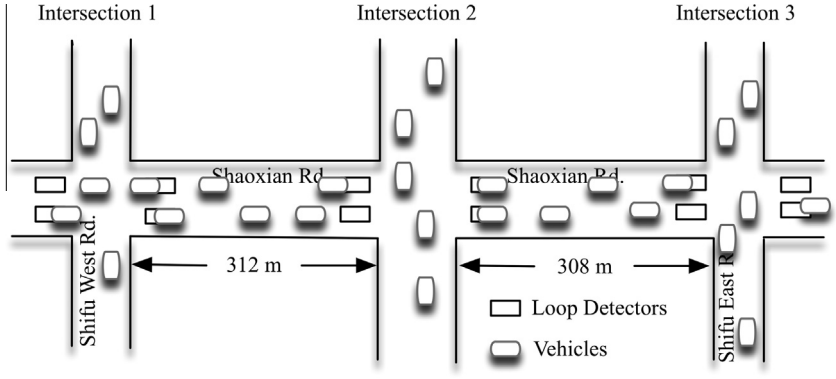

Fig. 2. The locations of loop detectors.

Table 1
Descriptive statistics of traffic volume data set.

Intersection	Amount	V_{max}	V_{min}	Mean	Standard deviation	Skewness	Observation period
1	128	603	32	316.66	177.59	-0.02	From 2012-9-17 19:00 to 2012-9-19 2:45
2	128	445	16	180.29	119.11	0.3	From 2012-9-17 19:00 to 2012-9-19 2:45
3	128	321	12	171.09	96.36	-0.16	From 2012-9-17 19:00 to 2012-9-19 2:45

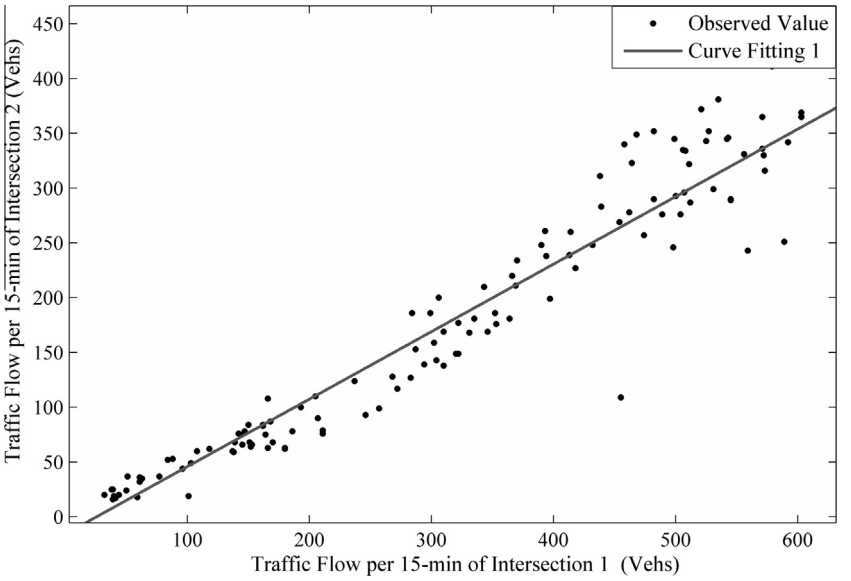

Fig. 3. Correlation diagram of Intersection 2 versus Intersection 1 traffic volume values.

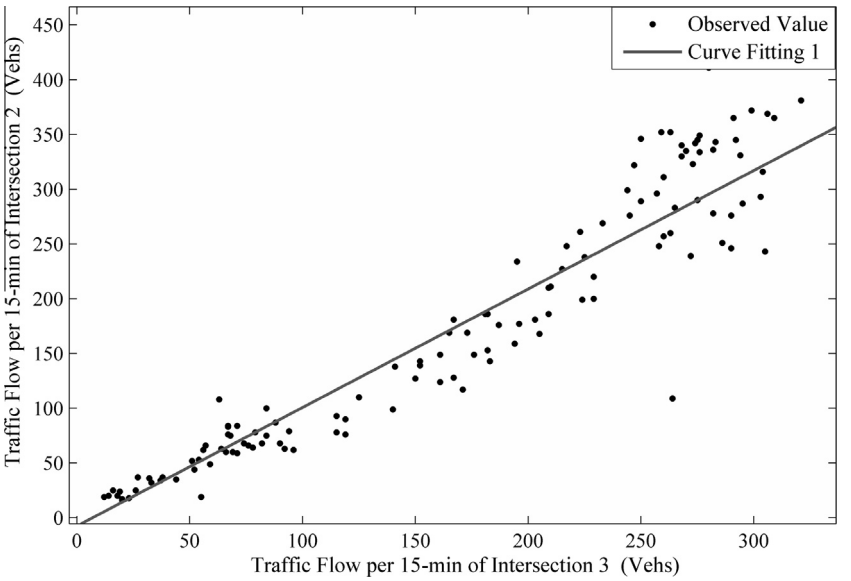

Fig. 4. Correlation diagram of Intersection 2 versus Intersection 3 traffic volume values.

training set to build the network, and the other 25 groups are used to test the network. For the first experiment, the input data are from a single intersection, while all 3 intersections' data are used as the input data for the second experiment.

Input 1: $\mathbf{x}_1(t) = \mathbf{v}_1^{\mathrm{T}}(t)$
Input 2: $\mathbf{x}_2(t) = (\mathbf{v}_1(t), \mathbf{v}_2(t), \mathbf{v}_3(t))^{\mathrm{T}}$

Table 2
Results of the goodness of fit (with 95% confidence bounds).

Curve Fitting	Equation	*SSE*[a]	R^2	Adjusted R^2	*RMSE*[b]
1	$V_2(i) = 0.6161 \cdot V_1(i) - 15.81$	4494	0.9975	0.9975	5.972
2	$V_2(i) = 1.082 \cdot V_3(i) - 7.453$	6259	0.9965	0.9965	7.048

[a] *SSE* is the sum of squares for error.
[b] *RMSE* denotes the root mean-square deviation.

Table 3
The Pearson Correlation Coefficient of each two intersections.

Intersection k_2–k_i	Pearson Correlation Coefficient
2–1	0.959
2–3	0.941

where $\mathbf{v}_1(t) = (v_1(t-45), v_1(t-30), v_1(t-15))$, $\mathbf{v}_2(t) = (v_2(t-45), v_2(t-30), v_2(t-15))$, and $\mathbf{v}_3(t) = (v_3(t-45), v_3(t-30), v_3(t-15))$.

In order to get more accurate results, data are normalized by Eq. (3):

$$x(i) = \frac{V_k(i) - V_k^{\max}}{V_k^{\max} - V_k^{\min}}, \quad i = 1, 2, \cdots, n;\ k = 1, 2, 3 \tag{3}$$

To get the final results, data can by anti-normalized by Eq. (4):

$$a = V_2(i)\left(V_2^{\max} - V_2^{\min}\right) + V_2^{\min}, \quad i = 1, 2, \cdots, n \tag{4}$$

where:

x = the input data of the neural network;
a = the final output of the neural network;
$V_k^{\max}$ = the maximum traffic flow at Intersection k during the entire observation period; and
$V_k^{\min}$ = the minimum traffic flow at Intersection k during the entire observation period.

We used the function $newrb(P, T, goal, spread, MN, DF)$ to design the RBFNN in MATLAB 2013a, where:

P = R-by-Q matrix of Q input vectors;
T = S-by-Q matrix of Q target class vectors;
goal = mean squared error goal (default = 0.0)
spread = spread of radial basis functions (default = 1.0);
MN = maximum number of neurons in hidden layer (default is Q);
DF = number of neurons to add between displays (default = 25).

Several tests have been done for obtain more accurate result based the existing data sets. And the parameters of the model were selected as Table 4 shows. The computational results are shown in Figs. 5 and 6, respectively. It is easy to find that Fig. 5 shows obvious time-lag phenomena in most the prediction points. And the figure of forecasting by using 3-intersection volume data shows less time-lag phenomena.

3.3. Performance evaluation

To evaluate the performance of the proposed approach with respect to the forecasting accuracy, various effective measures are applied, namely the mean absolute deviation, the mean absolute percentage error, and the root-mean-square deviation.

Table 4
Model specifications.

Parameters	1-Intersection	3-Intersection
R	3	9
S	1	1
Q	100	100
Hidden layers	1	1
Goal	0.001	0.001
Spread	2000	2000
MN	2	8
DF	Default	Default

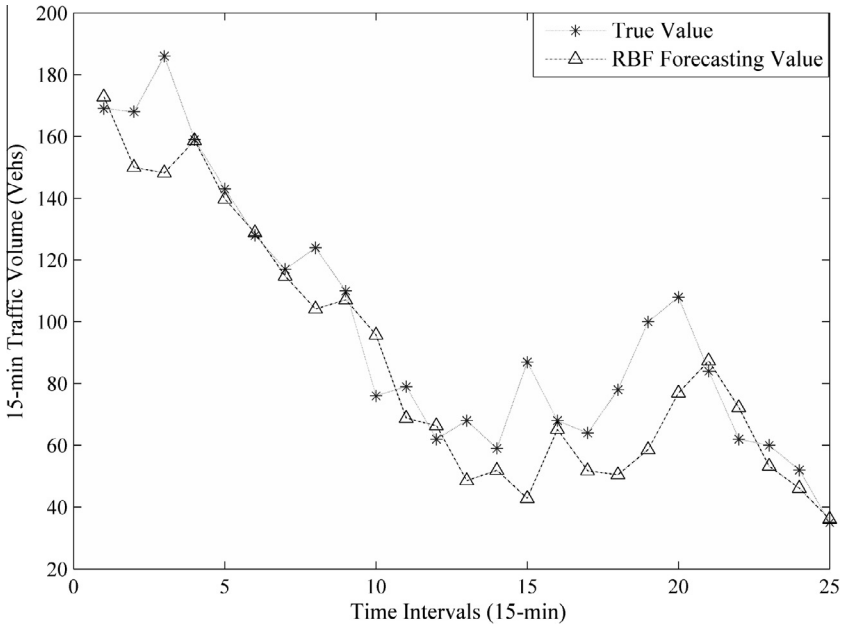

Fig. 5. Example of forecasting using 1-intersection data.

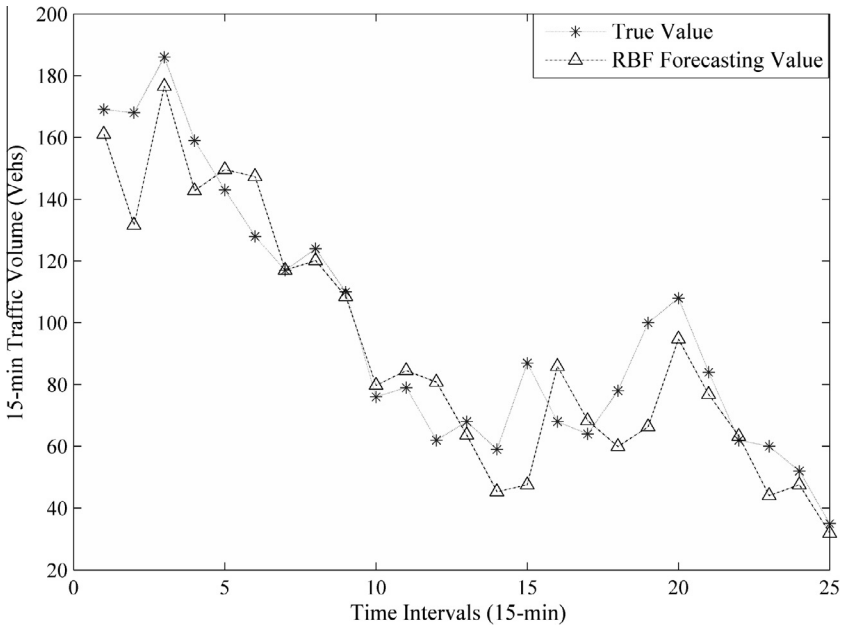

Fig. 6. Example of forecasting using 3-intersections data.

$$MAD = \frac{\sum_{i=1}^{n}\left|\widehat{V}_2(i) - V_2(i)\right|}{n}, \quad i = 1, 2, \cdots, n \tag{5}$$

$$MAPE = \frac{\sum_{i=1}^{n}\left|\frac{\widehat{V}_2(i) - V_2(i)}{V_2(i)}\right|}{n}, \quad i = 1, 2, \cdots, n \tag{6}$$

$$RMSE = \sqrt{\frac{\sum_{i=1}^{n}\left[\widehat{V}_2(i) - V_2(i)\right]^2}{n}}, \quad i = 1, 2, \cdots, n \tag{7}$$

where

MAD = mean absolute deviation;
MAPE = mean absolute percentage error;
RMSE = root-mean-square deviation;
$\widehat{V}_2(i)$ = the predicted traffic volume at Intersection 2 of Period i; and
$V_2(i)$ = the observed traffic volume at Intersection 2 of Period i.

From the results shown in Table 5, it can be observed that the result of using 3-intersection data outperforms the results using 1-intersection data. It shows that more related input vectors of RBFNN could improve the performance obviously. That is to say, using the traffic volume of adjacent intersection as the input of neural networks could improve the forecasting accuracy to some degree.

3.4. Relationship between the input vectors and the forecast accuracy

From the forecasting experiment above, we can conclude that using different input vectors of NN affect the forecast accuracy. This phenomenon inspired us to do more experiments to explore how the number and source of input vectors affect the accuracy. The input vector of Intersection 2 (Shaoxian Rd. & Aerding Ave.) remains unchanged. And the numbers of input vector of Intersection 1 (Shaoxian Rd. & Shifu West Rd.) and the right one (Shaoxian Rd. & Shifu East Rd.) are adjusted to test forecast accuracy. The vectors of both intersections are ranged from 0 to 3. So we obtain 16 groups of forecast results. Tables 6–8 show the performance evaluation of the tests.

From the performance evaluation above, we find most of result of the forecasting test shows the models using the traffic volume of adjacent intersections as input vectors outperform the original one. And sensitivity analyses for different input vectors with *MAPE*, *MAD* and *RMSE* were made as Figs. 7–9 shows. The accuracies of all the measures show the similar trend. Forecasting with the traffic volume $v_1(t-15), v_1(t-30)$ as additional input vectors can increase the accuracy obviously. Nevertheless, not all the additional input vectors can obtain better result. Using the traffic volume of Intersection 3 singly will bring worse accuracy of forecasting.

3.5. A performance comparison with ARIMA (ARIMAX) model

Inspired by the forecasting experiment, we speculate that using the same method will improve the forecasting accuracy of parametric models as well. Based on the same traffic volume data, we built two ARIMA models with the Expert Modeler of SPSS 22.0. First, we built an ARIMA (0, 1, 0) model based on the single time series of Intersection 2. Second, we built another ARIMA (0, 1, 1) model with two other time series of the adjacent intersections as the independent variables for the forecasting model, namely autoregressive integrated moving average with exogenous variables (ARIMAX). A comparison of forecast performance was shown in Table 9.

As can be seen from Table 9, Figs. 10 and 11, the forecasting accuracy is improved significantly and the time-lag phenomenon is mitigated to a certain degree. However, based on this method and data set, the RBFNN model obtains better forecasting accuracy.

4. A new method for missing-data traffic flow forecasting

In practical real-time traffic flow forecasting, data from loop detectors are always discontinuous due to the physical damage or the maintenance of loops and other roadside equipments. Davis and Nihan (1984) used time-series regression analyses to deal with missing data. Chen et al. (2001) developed two hybrid approaches using Self-Organizing Map with ARIMA and MLP for missing data traffic forecasting. Zhong et al. (2004) compared the performances of methods for estimation of missing traffic counts by using factor, genetic, neural, and regression. Van Lint et al. (2005) proposed a method of state-space neural network to deal with the situation with missing data. Zhong and Sharma's research proposed (2009) the improved imputation methods based on data from both before and after the failure and correction factor for missing traffic volume counts.

In this paper, we developed a simple method by using the traffic volume data at the adjacent intersections as the supplement input of NN. Manual data processing was done as some traffic volume was chosen as the missing one. The data used for the forecasting is listed in Table A.2. The input data are from a single intersection for the first experiment. And all 3

Table 5
Performance comparison of *MAPE*, *MAD*, and *RMSE* for two examples of forecasting.

	MAPE	*MAD*	*RMSE*
1-Intersection	0.1477	13.4505	18.8305
3-Intersection	0.1358	12.2342	16.2995

Table 6
Perfomance evaluation of tests using the *MAPE*[a].

Numbers of input vectors of Intersection 1	Numbers of input vectors of Intersection 3			
	0	1	2	3
0	0.1477	0.1655	0.1659	0.1633
1	0.1221	0.1457	0.1294	0.1263
2	0.1225	0.13	0.1265	0.1254
3	0.1423	0.1412	0.1358	0.1358

[a] *Notes:* 0 means no additional input vectors; 1 means the additional input vector is $v_k(t-15)$; 2 means the additional input vectors are $v_k(t-15)$, $v_k(t-30)$; 3 means the additional input vectors are $v_k(t-15)$, $v_k(t-30)$, $v_k(t-45)$.

Table 7
Perfomance evaluation of tests using the *MAD*.

Numbers of input vectors of Intersection 1	Numbers of input vectors of Intersection 2			
	0	1	2	3
0	13.4505	15.4886	15.5142	15.1846
1	11.0911	13.505	11.8569	11.7183
2	10.8989	11.914	11.1541	11.4471
3	12.3684	12.5712	12.2373	12.2342

Table 8
Perfomance evaluation of tests using the *RMSE*.

Numbers of input vectors of Intersection 1	Numbers of input vectors of Intersection 2			
	0	1	2	3
0	18.8305	20.702	20.6943	21.6084
1	15.2152	18.0633	16.4232	16.2113
2	14.2566	16.0143	14.8952	15.6442
3	15.7115	16.5382	16.3266	16.2995

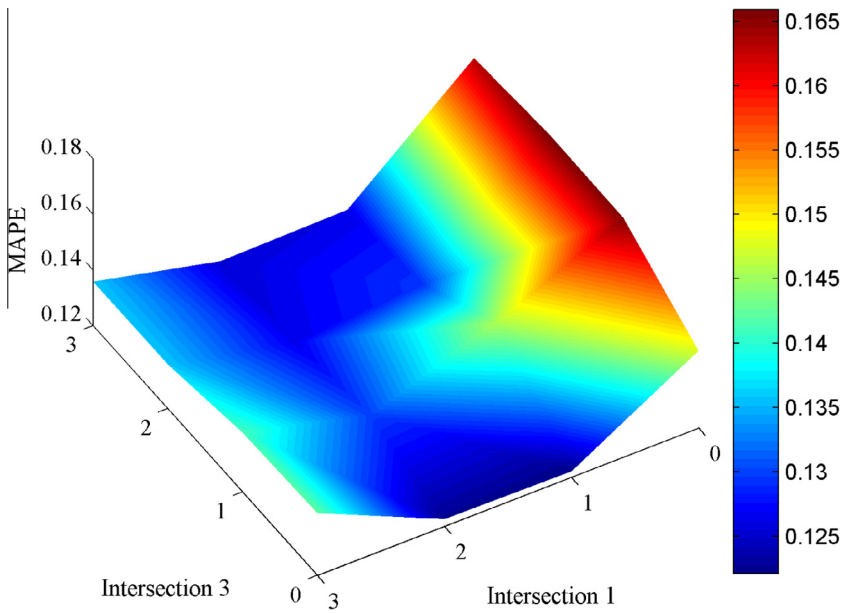

Fig. 7. Sensitivity analysis for different input vectors with *MAPE*.

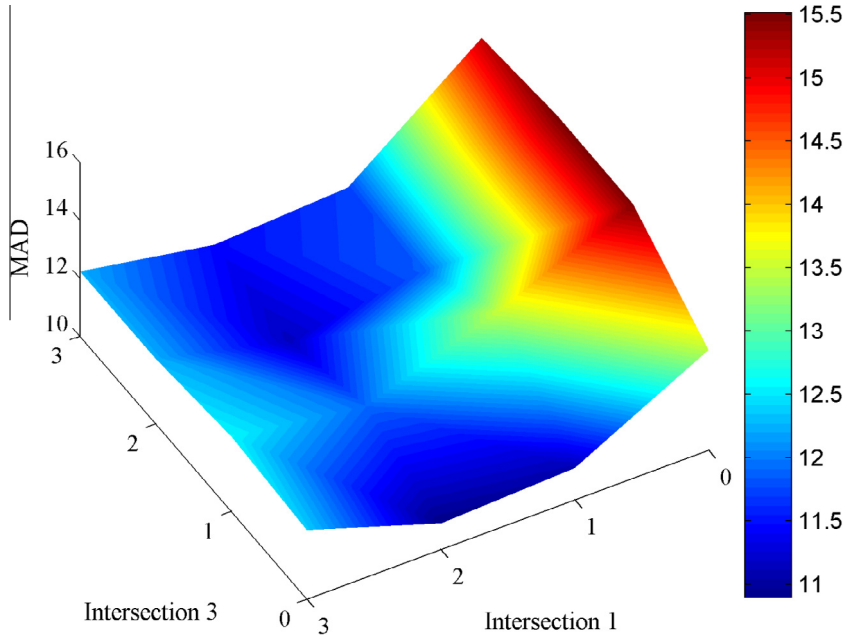

Fig. 8. Sensitivity analysis for different input vectors with *MAD*.

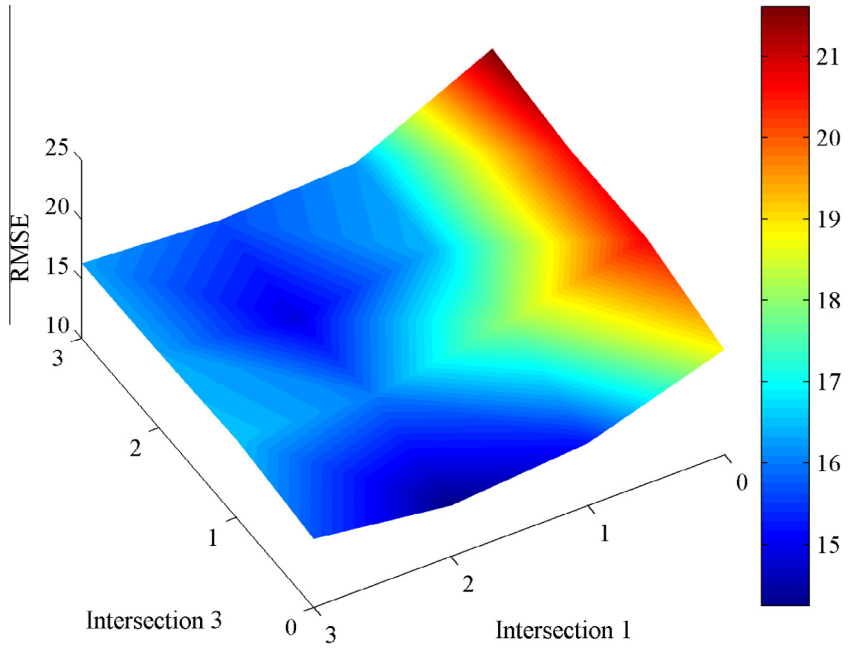

Fig. 9. Sensitivity analysis for different input vectors with *RMSE*.

Table 9
Performance comparison of *MAPE*, *MAD*, and *RMSE* for two examples of forecasting.

	MAPE	*MAD*	*RMSE*
1-Intersection	0.1784	15.1080	17.6069
3-Intersection	0.1343	13.2464	16.3948

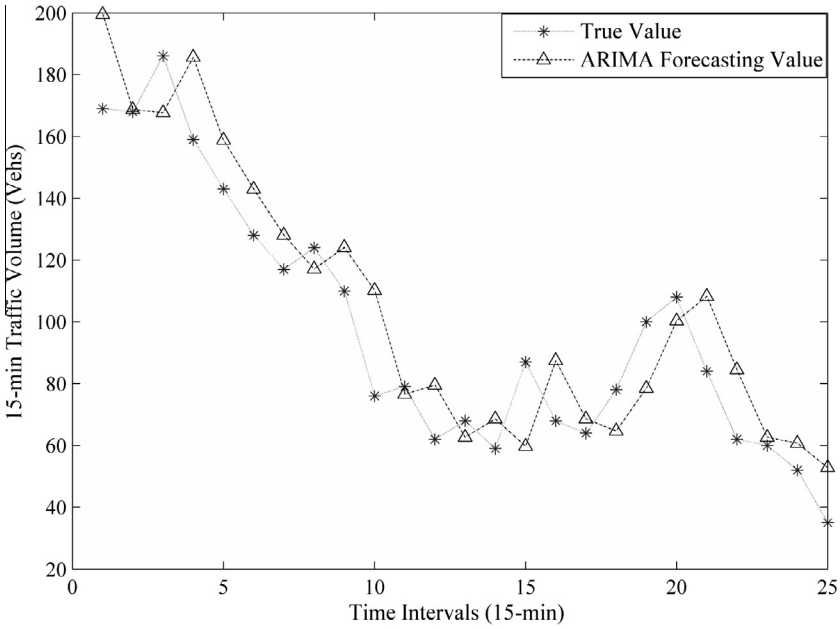

Fig. 10. Example of forecasting based on ARIMA model using 1-intersection data.

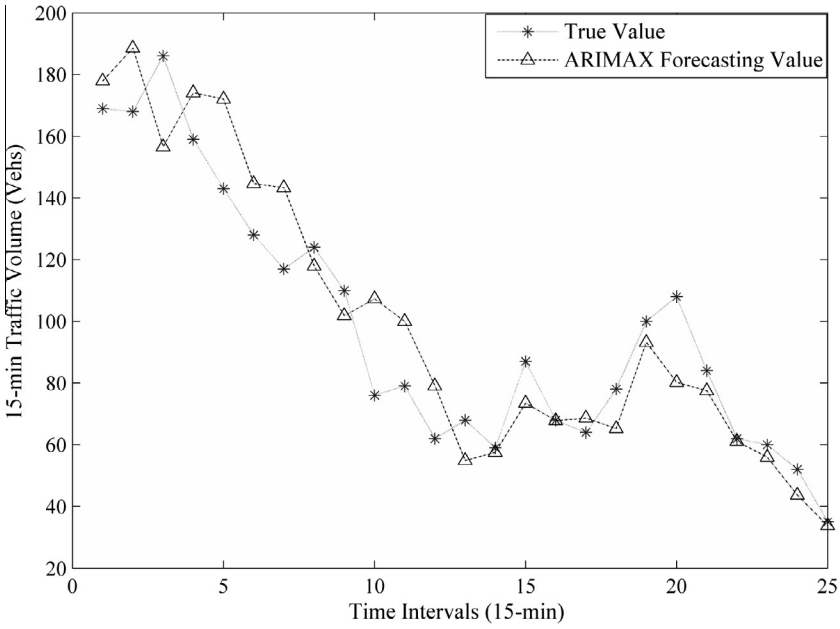

Fig. 11. Example of forecasting based on ARIMAX model using 3-intersections data.

intersections' data are used as the input data for the second experiment. The parameters of the NN model are the same with Section 3.1. And we compared the performance of both two experiments as Table 10 shows.

Input 1: $\mathbf{x}_1(t) = \mathbf{v}_1^{\mathrm{T}}(t)$
Input 2: $\mathbf{x}_2(t) = (\mathbf{v}_1(t), \mathbf{v}_2(t), \mathbf{v}_3(t))^{\mathrm{T}}$

where $\mathbf{v}_1(t) = (v_1(t-45), v_1(t-30), v_1(t-15))$, $\mathbf{v}_2(t) = (v_2(t-45), v_2(t-30), v_2(t-15))$, and $\mathbf{v}_3(t) = (v_3(t-45), v_3(t-30), v_3(t-15))$.

Table 10
Performance comparison for missing-data forecasting.

	MAPE	*MAD*	*RMSE*
1-Intersection	0.1896	16.7406	20.3948
3-Intersection	0.1583	14.9829	18.8601

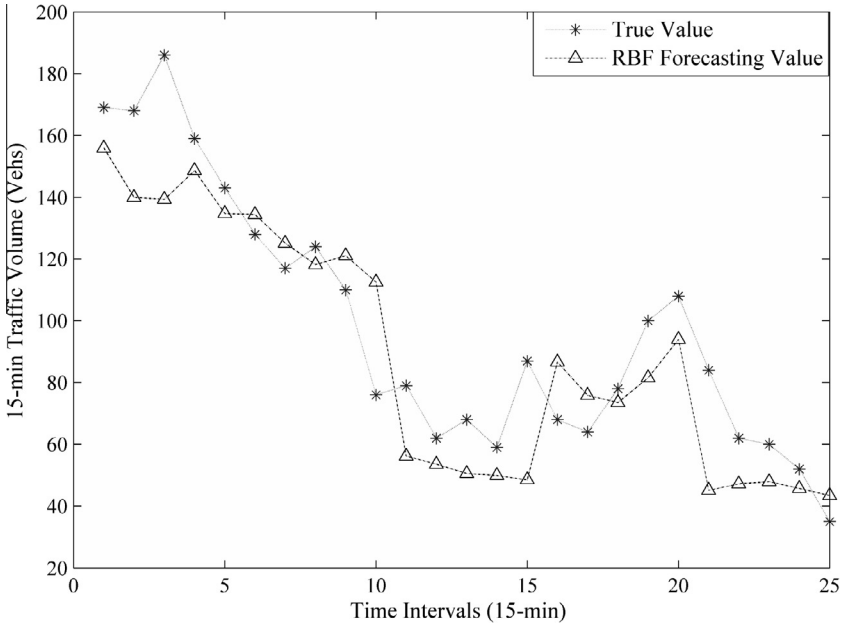

Fig. 12. Example of forecasting using 1-intersection data.

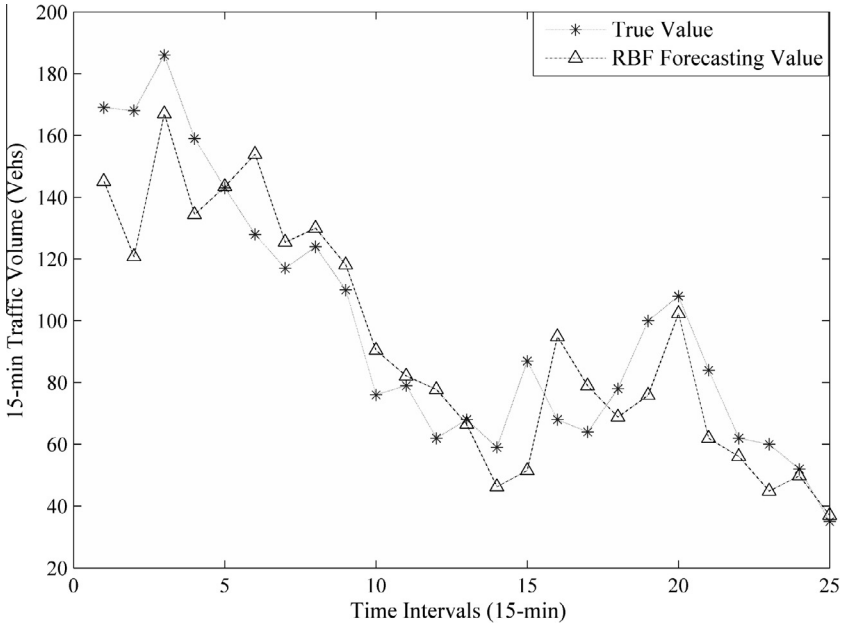

Fig. 13. Example of forecasting using 3-intersection data.

The performance comparison shows that the result of the improved model is more accurate. And the forecasting results are more meaningful (Figs. 12 and 13). Using traffic volume data of the adjacent intersections as the input data instead can obtain better forecasting results when the data at the intersection for forecasting are missed. Therefore, this method is more effective and can improve the robustness of the forecasting system.

5. Conclusion

In this paper, a new method based on RBF neural network is established to predict the short-team traffic volume. Traffic flows of one single intersection are significantly affected by the traffic flows at the adjacent intersections. It is proved by performing curve fitting of the traffic volume at the adjacent two intersections and by analyzing the two groups of traffic volume data. The results of the experiments show that the accuracy of forecasting by the proposed model is increased obviously.

Moreover, the correlation of traffic volume at two adjacent intersections shows that the traffic volume at adjacent intersections to some degree can replace the traffic volume at one intersection. This method provides a new idea to solve the problem of missing data in real-time traffic flow forecasting.

A further insight gained from this research is that the traffic flow at the adjacent intersections affects each other, not only in the traffic volume, but also in other parameters such as speed and density. Using the traffic data of the adjacent intersections to obtain more accurate forecasting result could be further studied.

Acknowledgements

This work is supported by the National Natural Science Foundation of China (Grant no. 712620), the Scientific Research Foundation for the Returned Overseas Chinese Scholars, State Education Ministry of China, and Program for Young Talents of Science and Technology in Universities of Inner Mongolia Autonomous Region, China (Grant no. NJYT-13-B02).

Appendix A

See Tables A.1 and A.2

Table A.1
Original traffic volume data (Vehs).

Time	Intersection 1	Intersection 2	Intersection 3
2012-9-17 19:00	573	316	304
2012-9-17 19:15	462	278	282
2012-9-17 19:30	454	269	233
2012-9-17 19:45	432	248	217
2012-9-17 20:00	397	199	224
2012-9-17 20:15	366	220	229
2012-9-17 20:30	352	186	181
2012-9-17 20:45	322	177	196
2012-9-17 21:00	346	169	173
2012-9-17 21:15	353	176	187
2012-9-17 21:30	304	143	152
2012-9-17 21:45	320	149	176
2012-9-17 22:00	310	138	141
2012-9-17 22:15	283	127	150
2012-9-17 22:30	294	139	152
2012-9-17 22:45	257	99	140
2012-9-17 23:00	246	93	115
2012-9-17 23:15	207	90	119
2012-9-17 23:30	186	78	115
2012-9-17 23:45	180	63	92
2012-9-18 0:00	170	68	74
2012-9-18 0:15	162	84	71
2012-9-18 0:30	166	63	64
2012-9-18 0:45	153	66	76
2012-9-18 1:00	137	60	69
2012-9-18 1:15	162	83	67
2012-9-18 1:30	144	75	68
2012-9-18 1:45	142	76	67
2012-9-18 2:00	145	66	57
2012-9-18 2:15	101	19	55
2012-9-18 2:30	88	53	54
2012-9-18 2:45	96	44	52

(*continued on next page*)

Table A.1 (*continued*)

Time	Intersection 1	Intersection 2	Intersection 3
2012-9-18 3:00	77	37	38
2012-9-18 3:15	62	34	37
2012-9-18 3:30	61	36	32
2012-9-18 3:45	50	24	19
2012-9-18 4:00	40	19	12
2012-9-18 4:15	38	25	26
2012-9-18 4:30	32	20	18
2012-9-18 4:45	44	20	14
2012-9-18 5:00	39	25	16
2012-9-18 5:15	39	16	20
2012-9-18 5:30	59	18	23
2012-9-18 5:45	41	17	20
2012-9-18 6:00	61	32	33
2012-9-18 6:15	51	37	27
2012-9-18 6:30	103	49	59
2012-9-18 6:45	164	75	84
2012-9-18 7:00	287	153	182
2012-9-18 7:15	322	149	161
2012-9-18 7:30	418	227	215
2012-9-18 7:45	527	352	263
2012-9-18 8:00	602	426	247
2012-9-18 8:15	603	369	306
2012-9-18 8:30	547	445	300
2012-9-18 8:45	500	293	303
2012-9-18 9:00	543	346	250
2012-9-18 9:15	498	246	290
2012-9-18 9:30	504	276	245
2012-9-18 9:45	507	296	257
2012-9-18 10:00	556	331	294
2012-9-18 10:15	506	335	270
2012-9-18 10:30	592	342	274
2012-9-18 10:45	531	299	244
2012-9-18 11:00	571	336	282
2012-9-18 11:15	579	411	280
2012-9-18 11:30	603	365	291
2012-9-18 11:45	559	243	305
2012-9-18 12:00	589	251	286
2012-9-18 12:15	521	372	299
2012-9-18 12:30	545	290	275
2012-9-18 12:45	413	239	272
2012-9-18 13:00	370	234	195
2012-9-18 13:15	335	181	203
2012-9-18 13:30	299	186	209
2012-9-18 13:45	364	181	167
2012-9-18 14:00	343	210	209
2012-9-18 14:15	393	261	223
2012-9-18 14:30	474	257	260
2012-9-18 14:45	499	345	275
2012-9-18 15:00	545	289	250
2012-9-18 15:15	482	290	275
2012-9-18 15:30	482	352	259
2012-9-18 15:45	468	349	276
2012-9-18 16:00	458	340	268
2012-9-18 16:15	464	323	273
2012-9-18 16:30	439	283	265
2012-9-18 16:45	438	311	260
2012-9-18 17:00	511	322	247
2012-9-18 17:15	508	334	276
2012-9-18 17:30	525	343	283
2012-9-18 17:45	542	345	292
2012-9-18 18:00	535	381	321
2012-9-18 18:15	571	365	309
2012-9-18 18:30	572	330	268
2012-9-18 18:45	512	287	295
2012-9-18 19:00	489	276	290
2012-9-18 19:15	414	260	263
2012-9-18 19:30	455	109	264
2012-9-18 19:45	390	248	258
2012-9-18 20:00	394	238	225

Table A.1 (*continued*)

Time	Intersection 1	Intersection 2	Intersection 3
2012-9-18 20:15	369	211	210
2012-9-18 20:30	306	200	229
2012-9-18 20:45	310	169	165
2012-9-18 21:00	331	168	205
2012-9-18 21:15	284	186	182
2012-9-18 21:30	302	159	194
2012-9-18 21:45	304	143	183
2012-9-18 22:00	268	128	167
2012-9-18 22:15	272	117	171
2012-9-18 22:30	237	124	161
2012-9-18 22:45	205	110	125
2012-9-18 23:00	211	76	119
2012-9-18 23:15	211	79	94
2012-9-18 23:30	180	62	96
2012-9-18 23:45	139	68	82
2012-9-19 0:00	138	59	71
2012-9-19 0:15	168	87	88
2012-9-19 0:30	151	68	90
2012-9-19 0:45	152	64	78
2012-9-19 1:00	147	78	79
2012-9-19 1:15	193	100	84
2012-9-19 1:30	166	108	63
2012-9-19 1:45	150	84	67
2012-9-19 2:00	118	62	56
2012-9-19 2:15	108	60	66
2012-9-19 2:30	84	52	51
2012-9-19 2:45	63	35	44

Table A.2
Manual processing of missing data (Intersection 2 Only, Vehs).

$V_2(t-45)$	$V_2(t-30)$	$V_2(t-15)$	Target
N/A	211	200	169
N/A	200	169	168
N/A	169	168	186
N/A	168	186	159
N/A	186	159	143
186	N/A	143	128
159	N/A	128	117
143	N/A	117	124
128	N/A	124	110
117	N/A	110	76
124	110	N/A	79
110	76	N/A	62
76	79	N/A	68
79	62	N/A	59
62	68	N/A	87
N/A	N/A	87	68
N/A	N/A	68	64
N/A	N/A	64	78
N/A	N/A	78	100
N/A	N/A	100	108
78	N/A	N/A	84
100	N/A	N/A	62
108	N/A	N/A	60
84	N/A	N/A	52
62	N/A	N/A	35

References

Abdulhai, B., Porwal, H., Recker, W., 1999. Short-term freeway traffic flow prediction using genetically-optimized time-delay-based neural networks. In: Proceedings of the Transportation Research Board 78th Annual Meeting.

Ahmed, M.S., Cook, A.R., 1979. Analysis of freeway traffic time-series data by using Box-Jenkins techniques. Transp. Res. Rec. 722, 1–9.

Amin, S.M., Rodin, E.Y., Liu, A.P., Rink, K., García-Ortiz, A., 1998. Traffic prediction and management via RBF neural nets and semantic control. Comput.-Aided Civil Infrastruct. Eng. 13 (5), 315–327.

Carrillo, J.A., Fornasier, M., Toscani, G., Vecil, F., 2010. Particle, kinetic, and hydrodynamic models of swarming. Math. Model. Collective Behav. Socio-Econ. Life Sci., 297–336.
Chen, H., Grant-Muller, S., Mussone, L., Montgomery, F., 2001. A study of hybrid neural network approaches and the effects of missing data on traffic forecasting. Neural Comput. Appl. 10 (3), 277–286.
Davis, G.A., Nihan, N.L., 1984. Using time-series designs to estimate changes in freeway level of service, despite missing data. Transp. Res. Part A 18 (5), 431–438.
Davis, G.A., Niham, N.L., Hamed, M.M., Jacobson, L.N., 1991. Adaptive forecasting of freeway traffic congestion. Transp. Res. Rec. 1287, 29–33.
Dia, H., 2001. An object-oriented neutral network approach to short-term traffic forecasting. Eur. J. Oper. Res. 131, 253–261.
Hamed, M.M., Al-Masaeid, H.R., Bani Said, Z.M., 1995. Short-term prediction of traffic volume in urban arterials. J. Transp. Eng. 121 (3), 249–254.
Helbing, D., 2001. Traffic and related self-driven many-particle systems. Rev. Mod. Phys. 73 (4), 1067.
Jayawardena, A.W., Fernando, D.A.K., 1998. Use of radial basis function type artificial neural networks for runoff simulation. Comput.-Aided Civil Infrastruct. Eng. 13 (2), 91–99.
Kamarianakis, Y., Prastacos, P., 2003. Forecasting traffic flow conditions in an urban network: comparison of multivariate and univariate approaches. Transp. Res. Rec. 1857, 74–84.
Karlaftis, M.G., Vlahogianni, E.I., 2011. Statistical methods versus neural networks in transportation research: differences, similarities and some insights. Transp. Res. Part C 19 (3), 387–399.
Levin, M., Tsao, Y.D., 1980. On forecasting freeway occupancies and volumes. Transp. Res. Rec. 773, 47–49.
Li, Y.X., Lukeman, R., Edelstein-Keshet, L., 2008. Minimal mechanisms for school formation in self-propelled particles. Physica D 237 (5), 699–720.
Lin, S., Xi, Y., & Yang, Y., 2008. Short-term traffic flow forecasting using macroscopic urban traffic network model. In: Proceedings of the 11th International IEEE Conference on Intelligent Transportation Systems.
Park, B., Messer, C.J., Urbanik II, T., 1998. Short-term freeway traffic volume forecasting using radial basis function neural network. Transp. Res. Rec. 1651, 39–47.
Park, B.B., 2002. Hybrid neuro-fuzzy application in short-term freeway traffic volume forecasting. Transp. Res. Rec. 1802, 190–196.
Reynolds, C.W., 1987. Flocks, herds and schools: a distributed behavioral model. ACM SIGGRAPH Comput. Graphics 21 (4), 25–34.
Ripley, B.D., 1993. Statistical aspects of neural networks. In: Networks and Chaos—Statistical and Probabilistic Aspects. Chapman & Hall, London, pp. 40–123.
Ripley, B.D., 1994. Neural networks and related methods for classification (with discussion). J. R. Stat. Soc. B 56 (3), 409–456.
Stathopoulos, A., Karlaftis, M.G., 2003. A multivariate state-space approach for urban traffic flow modelling and prediction. Transp. Res. Part C 11 (2), 121–135.
Stathopoulos, A., Karlaftis, M.G., 2001. Temporal and spatial variations of real-time traffic data in urban areas. Transp. Res. Rec. 1768, 135–140.
Toner, J., Tu, Y., 1995. Long-range order in a two-dimensional dynamical XY model: how birds fly together. Phys. Rev. Lett. 75 (23), 4326.
Van der Voort, M., Dougherty, M., Watson, S., 1996. Combining Kohonen maps with ARIMA time-series models to forecast traffic flow. Transp. Res. Part C 4 (5), 307–318.
Van Lint, J.W.C., Hoogendoorn, S.P., van Zuylen, H.J., 2005. Accurate freeway travel time prediction with state-space neural networks under missing data. Transp. Res. Part C 13 (5), 347–369.
Vlahogianni, E.I., Golias, J.C., Karlaftis, M.G., 2004. Short-term traffic forecasting: overview of objectives and methods. Transport Rev. 24 (5), 533–557.
Vlahogianni, E.I., Karlaftis, M.G., Golias, J.C., 2005. Optimized and meta-optimized neural networks for short-term traffic flow prediction: a genetic approach. Transp. Res. Part C 13 (3), 211–234.
Vlahogianni, E.I., Karlaftis, M.G., Golias, J.C., 2008. Temporal evolution of short-term urban traffic flow: a nonlinear dynamics approach. Comput.-Aided Civil Infrastruct. Eng. 23 (7), 536–548.
Whittaker, J., Garside, S., Lindveld, K., 1997. Tracking and predicting a network traffic process. Int. J. Forecast. 13 (1), 51–61.
Williams, B.M., 2001. Multivariate vehicular traffic flow prediction: evaluation of ARIMAX modeling. Transp. Res. Rec. 1776, 194–200.
Williams, B.M., Hoel, L.A., 2003. Modeling and forecasting vehicular traffic flow as a seasonal ARIMA process: theoretical basis and empirical results. J. Transp. Eng. 129 (6), 664–672.
Yin, H., Wong, S.C., Xu, J., 2002. Urban traffic flow prediction using fuzzy-neural approach. Transp. Res. Part C 10 (2), 85–98.
Zheng, W., Lee, D.H., Shi, Q., 2006. Short-term freeway traffic flow prediction: Bayesian combined neural network approach. J. Transp. Eng. 132 (2), 114–121.
Zhong, M., Sharma, S., 2009. Development of improved models for imputing missing traffic counts. Open Transp. J. 3, 35–48.
Zhong, M., Lingras, P., Sharma, S., 2004. Estimation of missing traffic counts using factor, genetic, neural, and regression techniques. Transp. Res. Part C 12 (2), 139–166.